Slow Steady-Shear of Plastic Bead Rafts

Michael Twardos and Michael Dennin

Abstract Experimental measurements of the response of a two dimensional system of plastic beads subjected to steady shear are reported. The beads float at the surface of a fluid substrate and are subjected to a slow, steady-shear in a Couette geometry. The flow consists of irregular intervals of solid-like, jammed behavior, followed by stress relaxations. We report on statistics that characterize the stress fluctuations as a function of several parameters including shear-rate and packing density. Over a range of densities between the onset of flow to the onset of buckling (overpacking) of the system, the probability distribution for stress fluctuations is essentially independent of the packing density, particle dispersity, and interaction potential (varied by changing the substrate). Finally, we compare the observed stress fluctuations with those observed in other complex fluids.

1

Introduction

For equilibrium systems, it is well understood how fluctuations are controlled by temperature. Especially important

is the understanding of the role of fluctuations in the modern theory of phase transitions [1]. Similarly, one expects nonequilibrium fluctuations to play an equally important role in transitions in driven systems, such as the proposed jamming transition as a function of external stress [2,3,4]. In driven systems, the fluctuations of interest are typically not thermal in nature. Instead, they are the result of the external driving, and this raises important questions and presents a number of challenges. As a starting point, it is useful to characterize the statistics of these "athermal" fluctuations and ask how similar such statistics are to equivalent measures of thermal fluctuations. Then, one can consider the impact athermal fluctuations on the system's dynamics.

A general feature of fluctuations in many driven systems is the occurrence of non-Gaussian features, typically an asymmetric shape with exponential tails, in probability distributions of the fluctuating quantity. It is interesting to ask under what conditions such distributions are *universal*. This question has been studied in the context of turbulent fluid flows for thermally driven fluids [5] (thermal convection) and electrically driven fluids [6,7] (electroconvection). More recent work has considered this question in shaken granular systems [8]. The focus in these studies has been on fluctuations in the dissipated power.

Two different approaches for characterizing fluctuations in the dissipated power were used. The first is based on the generalized fluctuation-dissipation theorem of Gallavotti and Cohen, also referred to as the Fluctuation-Theorem [9]. A key aspect of the FT theorem is the occurrence of rare negative fluctuations in power. This has been indirectly tested in fluid systems [5,6], and more recently direct measurements have been made in a shaken, granular system [8]. The second approach focuses on the form of the probability distribution function, or distribution function for short. One prediction is that the generalized Fisher-Tippit-Gumbel (gFTG) distribution function describes power fluctuations [10]. Experiments using electroconvection have demonstrated an interesting evolution of the distribution function from Gaussian behavior to behavior that is consistent with the gFTG distribution as the distance from equilibrium is varied [7].

Another class of systems that have been used heavily for the study of nonequilibrium fluctuations are soft-matter systems. A striking observation that arises from these studies is the similarity between the observations of fluctuations in foam [11,12,13,14,15], granular materials [16,17,18,8], and colloidal suspensions [19]. In the examples cited here, the fluctuations in stress under conditions of steady applied strain rate were studied. Similarities in various measures of the fluctuations exist despite qualitative differences in the "microscopic" structure of the materials. For example, foam consists of gas bubbles with liquid walls. For flowing foam, viscous dissipation in the fluid walls is the major source of energy loss. For comparison, the dissipation in granular systems is usually due to

dry friction between particles. Another potentially significant difference is the the degree to which the particles or bubbles are packed. Because of the solid nature of granular particles, they are generally studied at packing densities near or below random close packed. In contrast, foam "melts" at packing densities near random close packed, and studies focus on packing densities greater than the melting transition. Given these "microscopic" differences, it is worth commenting on some of the similarities that are observed in previous studies.

For foam, there is both a rich history of theoretical modelling [20,21,22,23,24,25,26,27,28] and experimental studies [11,12,14,15,13] that deals with the issue of fluctuations. The focus is on predicting the probability distribution of energy (or stress) drops, referred to as energy (stress) drop distributions. (Typically, simulations focus on energy drops because it is relatively easy to compute the total energy of the system. In contrast, experiments tend to focus on measurements of stress, as this is the more accessible quantity.) The focus on the energy (or stress) drop distributions was originally motivated by potential connections to self-organized criticality and the observation of power-law behavior [20]. In this context, the models of foam can be divided into two main classes: models that predict power-law distributions for stress or energy drops [20,21,22,23,24] and models that predict a definite average stress drop size [25,26,27,28]. Experimental evidence from model two-dimensional systems generally supports a distribution with a well-defined average [11,12,14,15]. However, there is indirect evidence for power-law distributions under conditions of quasi-static shear [13]. One issue

that has not been thoroughly explored in experiments is the possibility of the development of power-law behavior near the melting transition. There is some evidence in simulations exhibiting a well defined average energy drop that the average energy drop increases as one approaches the melting transition. This might indicate that the distribution is approaching a power law [28].

For granular materials, there have been limited measurements of stress drop distributions. Behavior similar to that observed in foam is reported for a system of elastic disks that are slowly sheared [18]. In general, the distribution is consistent with the existence of a characteristic size for the stress drops. The system reported on in Ref. [18] exhibits a continuous transition at which stress chains first extend across the system [17]. Near this transition point, there is evidence of possible power law behavior for the distribution of stress drops.

More commonly, the focus in granular systems has been on the probability distribution for the stress itself [16,17,8], as was also studied in colloidal systems [19]. (For the purposes of this paper, this will be referred to as the stress distribution, in contrast to the stress drop distribution.) For all of these systems, one surprising feature is how large the stress variations can be [16,19]. In one case, stress was measured normal to the flow in a localized region of the system. For different particle sizes, small variations in a general Maxwellian stress distribution were observed, but all of the distributions had essentially exponential tails for stress greater than the average stress [16]. The nature of the stress distributions appeared to depend strongly on the nature of the stress chains in the granular

material [16]. Another case measured stress distributions in a colloidal system as a function of strain rates. For low strain rates, gaussian distributions in stress were observed. For higher strain rates extreme value distribution statistics were measured with a well defined maximum value [19].

As a bridge between foam and granular systems, we have carried out studies of fluctuations using a modification of the bubble raft [29]: a bead raft (plastic beads floating on the surface of a fluid substrate). The plastic beads provide a connection with granular systems. However, their individual density is such that they are mostly submerged below the fluid substrate. Therefore, there is a fluid layer between the beads, analogous in some ways to the fluid walls in a foam. In this regard, the system is closest to a two-dimensional colloidal system. However, in contrast to typical colloidal systems used to study flow (see for example, Ref. [19]) the particles used here are much larger (mm in size), so thermal fluctuations play no role. Also, because the particles are only partially submerged, the role of the lubrication of the fluid subphase is not well understood yet.

The bead raft is essentially a two dimensional system with free boundary conditions perpendicular to the surface. The system has an easily adjustable dispersity, packing fraction, strain rate, and interaction potential. We report on measurements of stress during steady shear including average stress values (which determine the flow regime for a given strain rate), stress distributions, and stress drop distributions. By measuring both the stress and the stress drop distributions, we are able to make

comparisons with the stress drop distributions observed in foam and the stress distributions studies in granular matter. Using the stress distributions, we can make indirect comparison with the power dissipated distributions observed in turbulent flows.

2

Experimental Details

In our experiments, we use a centrosymmetric trough that can measure stress with a freely hanging torsion pendulum. This apparatus is described in detail in Ref. [30]. It consists of two concentric cylinders oriented vertically. The outer cylinder consists of 12 individual "fingers" that can be expanded and compressed between 6 and 12 cm to adjust the packing fraction of the beads. This barrier can be rotated in either direction at a constant angular speed in the range of 0.0005 rad/sec to 0.4 rad/sec. The inner cylinder is a Teflon rotor that "grips" the material by the insertion of eight 5 mm aluminum "paddles". The rotor has a diameter of 2.7 cm and is suspended by a torsion wire with a torsion constant, $\kappa = 3020$ dyne cm/rad. Induced voltage in a coil attached to the pendulum was used to determine the angle of the pendulum. When the outer barrier is rotated we can measure the torque on the inner cylinder and the corresponding stress on the inner cylinder. For the rest of the paper, unless otherwise indicated, the stress refers to the stress on the inner cylinder.

The system consists of spherical plastic beads localized to the surface of a fluid by their buoyancy. Their density is 0.95 g/cm^3, allowing each sphere to float at the fluid's surface. Unless noted, a bidisperse mixture of beads was used: 300 0.25 inch beads and 300 0.1875 inch beads. The simplest definition of packing fraction was used: the number of beads of each size times the maximal cross sectional area divided by the area of the system. At the highest compressions, this does not account for possible displacements perpendicular to the fluid surface. The system was thoroughly mixed and a disordered two dimensional system was created in the apparatus between the barriers. Because some signs of aging on short time scales were found, all measurements were performed after 1 hour of rotation in the same direction. Over the time scale of our experiments, we found no signs of coarsening or other settling phenomena common with some agitated polydisperse granular systems.

The substrates used ranged from pure water to pure glycerine, and included glycerine/water mixtures. The variation in substrate effectively changes the interaction between the beads because of changes in the properties of the fluid layer between particles. For all cases, coupling of the beads to the substrate was negligible. This was tested by removing the outer layer of beads from contact with the outer barrier. In this case, rotation of the outer barrier yielded zero stress on the inner rotor, and no motion of the beads was detected in this case.

For many of the experiments, the system was video taped to monitor the general behavior of the beads. Except for the highest packing fractions (as discussed below), there was no discernable motion of the beads out of the plane of the fluid surface. However, this does not completely rule out that some of the release of stress was due to slight motions of the beads in this direction. Such

releases in stress may be important if quantitative comparison with purely two-dimensional models are carried out in the future. However, for the main results of this paper, which is focused on the degree of *universality* of the fluctuations, the details of the source of stress release are not relevant.

3

Results

Figure 1 shows typical time series of the stress on the inner rotor as the outer barrier is rotated for three different packing fractions. The packing fractions were selected to illustrate three qualitatively different behaviors. For the lowest packing fraction (solid black line, lowest curve), the stress is predominately zero. This is due to the fact that under constant shear, the particles are driven toward the outer boundary. For sufficiently low densities, this results in exactly zero stress on the inner boundary, as no particles are in contact with it. As the packing fraction is increased, there is a density regime for which particles intermittently contact the inner rotor. This results in the occasional spikes in the stress.

The second behavior is illustrated by the red line (middle curve). This occurs when there are always particles in contact with the inner rotor, but the fluctuations occasionally result in the stress dropping back to zero. Finally, at high enough packing fraction (blue curve, highest average stress), the stress is always nonzero during the time for which the flow is observed. The rest of the results focus on the average stress value, the probability distribution of the stress, and the stress drop distributions, as calculated from time series similar to those illustrated in Fig. 1.

The first question that is addressed is the dependence of the average stress on the rotation rate and the density. Figure 2 presents the results for the average stress versus rotation rate for three different substrates. For all three cases, the behavior is consistent with that of a power law fluid. A power law fluid is one in which the viscosity, η, as a function of strain rate, $\dot{\gamma}$ is given by: $\eta \propto \dot{\gamma}^{(m-1)}$. For the Couette geometry, $\dot{\gamma} \propto \Omega$, where Ω is the outer rotation rate. This gives $<\sigma> = \eta\dot{\gamma} \propto \Omega^m$. From this, we find that for glycerine $m = 0.53 \pm 0.02$. For 70% glycerine 30% water mixture, $m = 0.35 \pm 0.02$, and for pure water, $m = 0.20 \pm 0.01$.

Before discussing these results further, it is useful to consider the average stress as a function of packing fraction, as illustrated in Fig. 3. For this system, there are a number of transitions as a function of packing fraction. As already discussed with regard to Fig. 1, for small enough packing fractions there is no transfer of stress between the inner and the outer barriers. The transition from this regime to non-zero average stress is somewhat poorly defined due to long-time transients. Figure 3 only covers densities for which the stress did not go to zero over experimental time scales of a few hours. The second transition is the "buckling" of the bead raft. This is indicated by the change in slope at higher packing fraction and is confirmed by imaging the bead raft.

Before the buckling transition occurs, the average stress as a function of density is consistent with a diverging power law, suggestive of an approach to the "jamming"

transition [2]. Therefore, for the range of density of interest (below buckling and with nonzero average stress), the system is below the jamming transition and should be in a purely fluid state. This is consistent with the results presented in Fig. 2, from which there is no evidence for a yield stress. In contrast, the bubble raft is above the jamming transition and clearly exhibits a yield stress [14, 15].

A critical packing fraction ρ_c for the jamming transition is determined by fitting the data to

$$\langle \sigma \rangle = \frac{\sigma_o}{(1 - (\rho/\rho_c))^n}. \tag{1}$$

The fits are given by the solid lines in Fig. 3. It should be noticed that this fit focuses on the divergence of the stress at higher packing fraction. This is opposite of the definition of the critical packing fraction reported in Ref. [17], where the interest was the initial transition to nonzero stress.

Figures 2 and 3 reveal a dependence of two characterizations of the average properties of the system on the choice of substrate: the exponent of the power-law viscosity (m) and the critical density for jamming (ρ_c). All of the data can be fit with the same exponent of the stress divergence $(n = 2)$. The general trend is for m to increase as the concentration of glycerine is increased, and for ρ_c to decrease as parameters are decreased. The values of m were already reported. For ρ_c, some examples are $\rho_c = 0.74$ and $\rho_c = 0.78$ for the pure glycerine and water substrates, respectively. An interesting feature of ρ_c is that it appears to be independent of rotation rate, even for the glycerine substrate. The dependence of the parameters

on substrate presumably reflects changes in the interactions between the beads due to the changing properties of the substrate. This is possible because the substrate coats a significant fraction of the beads and forms a thin film between particles. Therefore, it is reasonable to consider variations in substrate composition as variations in particle interactions.

Figure 4 displays the probability distribution for the stress for four different packing fractions on a water substrate. As the packing fraction increases, the average stress $(< \sigma >)$ and the variance in stress $(\delta \sigma)$ increase. Figure 5 shows normalized probability distributions, where we have plotted the probability of $(\sigma - < \sigma >)/\delta\sigma$ for a number of different situations. There are two striking features of the normalized distributions. First, for all of the parameter values for which we made measurements, the normalized distributions essentially collapse on a single curve. Second, the curve is asymmetric, with an exponential tail for stresses greater than the average stress.

In order to make comparisons with other work on stress distributions, we attempted to fit the data to three different models. The first model is based on the gFTG distribution function used to describes power fluctuations [10]:

$$\Pi(\sigma) = K(e^{x - e^x})^a, \tag{2}$$

where $x = b(\sigma - s)$ and $a = \pi/2$.

The parameters in this function are set by the criteria of unit area, zero mean, and unit variance. The plot in Fig. 5 uses values for the parameters that are expected based on Ref. [10]: $s = 0.37$ and $b = -0.94$. The only difference is that the constant b is negative because our

distribution is flipped with regard to the asymmetry measured in turbulent systems.

We also fit our plot to distributions of the form

$$P(\sigma) = (\sigma - \sigma^*)^2 e^{-(\sigma-\sigma^*)^n/<\sigma>} \tag{3}$$

for n = 1 and 2. These are chosen to compare with the results from Ref. [16] and a Maxwell-Boltzmann distribution, respectively. Here, σ^* was adjusted to get the best fit to the data. Not surprisingly, the gFTG distribution and distribution used in Ref. [16] best capture the exponential tail for high stress and provide the closest fit to the data.

Figure 6 shows the distribution of stress drops for three packing fractions. The general trend is similar to that observed for foam. There is an exponential cutoff in the stress drop distribution that results in a well-defined average stress drop. Unlike the normalized stress distribution, the average stress drop increases as one approaches the jamming transition from below. However, the average stress drop does not diverge as quickly as the average stress itself. Therefore, the average stress drop normalized by the average stress actually decreases as a function of density (see Fig. 7).

4

Discussion

We have presented results for the response of a plastic bead raft floating on a fluid substrate to the application of constant rate of strain. The system was selected to provide a bridge between similar studies in foam and granular materials by combining features of both materials, as more traditional collodial systems do. The system was

studied in a Couette geometry in which the outer cylinder was rotated at a constant angular speed and the stress on the inner cylinder was measured. A number of properties were measured as a function of packing fraction (or density), applied strain rate (or rotation rate), and interaction strength (or substrate composition). The main focus of the study was the behavior of the fluctuations in stress. In this regard, two quantities were characterized: the distribution of stress and the distribution of stress drops.

The results for the stress drop distributions are very similar to those found in foam [14,15] and granular material [18]. There is evidence for power-law behavior for small stress drops, but there is an exponential cutoff. The net result is a well-defined average stress drop. The average stress drop does increase as the packing fraction is increased, but not as fast as the average stress. There was no strong evidence for an approach to a power-law behavior at either the high or low critical densities. However, this might have been due to difficulties with approaching close enough to these transitions. For low packing fractions, the system became highly inhomogeneous, with beads concentrating toward the outer cylinder. At the high end, there was the cross-over to stress releases due to bead motion into the third dimension. Future work will be needed to explore the detailed behavior near these transitions.

With regard to the distribution of stress itself, some interesting "universal" features are observed. The most obvious feature is the exponential tail in the stress distribution that is consistent with observations in both granular systems [16] and highly driven fluids [7]. As with the driven fluid system, it is intriguing to note that the gFTG

distribution function, proposed in Ref. [10], is consistent with the data. The one difference is that the exponential tail in our data is for stress greater than the average stress. This is similar to the granular systems, in which stress is also the measured quantity [16]. This difference can be understood in terms of the connection between stress transmitted to the inner rotor and the power *dissipated* by the system. Because a constant power is input from the outer rotor, when the stress on the inner cylinder is higher than average, the power dissipated by the system is lower than average. Additional theoretical work is needed to fully understand why, and under what conditions, the gFTG distribution applies to this system. Also, it should be noted that there is still sufficient scatter in the data that it is not possible to rule out other distributions with exponential tails, such as the function used in Ref. [16].

One feature of the stress distributions that we were not able to access with our system was the extremely high strain rate limit. For colloids in this limit [19], the stress distribution developed an interesting structure that included a plateau. This behavior was never observed in our system. Future work will attempt to reach the necessary high strain rates, as the beads at the air-water interface is essentially a colloidal system.

Finally, the average stress was found to diverge as one approached a critical density as the density was increased at constant strain rate. This represents a diverging viscosity for the system. One way to understand this behavior is within the context of the proposed "jamming" transition [2,3,4]. Jamming is the crowding of constituent particles, disabling their kinetics and further exploration of phase space [2,3,4]. When a system develops a yield stress or extremely long relaxation time, it jams [31]. The jamming phase diagram proposes that one can approach the jammed state by either varying density, temperature, or shear stress [2]. An interesting feature of the jamming transition is that for finite size systems in the absence of shear, there is a distribution of critical densities that depend on the particle configurations [32,31,33]. An open question is how this distribution of jamming transitions impacts the behavior of the system under steady shear. It is easy to imagine that the shear causes the system to explore configuration space, randomly moving between jammed and unjammed states. This exploration of phase space would be a source of stress fluctuations. A future challenge is to understand the connection between the average stress, the fluctuations, and the distribution of jammed states. Future experiments exploring the impact of system size will be critical to answering this intriguing question.

References

1. A. Onuki, *Phase Transition Dynamics* (Cambridge University Press, 2002).

2. A. J. Liu, and S. R. Nagel, Nature **396**, (1998) 21.

3. V. Trappe, V. Prasad, L. Cipelletti, P. N. Segre, and D. A. Weitz, Nature **411**, (2001) 772.

4. A. J. Liu, and S. R. Nagel (eds.), *Jamming and Rheology: Constrained Dynamics on Microscopic and Macroscopic Scales* (Taylor and Francis Group, 2001).

5. S. Ciliberto, and C. Laroche, J. Phys. IV **8**, (1998) 215.

6. W. I. Goldburg, Y. Goldschmidt, and H. Kellay, Phys. Rev. Lett. **87**, (2001) 245502.

7. T. Toth-Katona, and J. T. Gleeson, Phys. Rev. Lett. **91**, (2003) 264501.

8. K. Feitosa, and N. Menon, (2003), cond-mat/0308212 .

9. G. Gallavotti, and E. G. D. Cohen, Phys. Rev. Lett. **74**, (1995) 2694.

10. S. T. Bramwell, K. Christensen, J.-Y. Fortin, P. C. W. Holdsworth, H. J. Jense, S. Lise, J. M. López, M. Nicodemi, J.-F. Pinton, and M. Sellitto, Phys. Rev. Lett. **84**, (2000) 3744.

11. A. D. Gopal, and D. J. Durian, Phys. Rev. Lett. **75**, (1995) 2610.

12. M. Dennin, and C. M. Knobler, Phys. Rev. Lett. **78**, (1997) 2485.

13. A. A. Kader, and J. C. Earnshaw, Phys. Rev. Lett. **82**, (1999) 2610.

14. J. Lauridsen, M. Twardos, and M. Dennin, Phys. Rev. Lett. **89**, (2002) 098303.

15. E. Pratt, and M. Dennin, Phys. Rev. E **67**, (2003) 051402.

16. B. Miller, C. O'Hern, and R. P. Behringer, Phys. Rev. Lett. **77**, (1996) 3110.

17. D. Howell, B. Behringer, and C. Veje, Phys. Rev. Lett. **82**, (1999) 5241.

18. R. R. Hartley, and R. P. Behringer, Nature **421**, (2003) 928.

19. D. Lootens, H. V. Damme, and P. Hébraud, Phys. Rev. Lett. **90**, (2003) 178301.

20. K. Kawasaki, T. Nagai, and K. Nakashima, Phil. Mag. B **60**, (1989) 399.

21. K. Kawasaki, T. Okuzono, T. Kawakatsu, and T. Nagai, 1992, in *Proc. Int. Workshop of Physics of Pattern Formation*, edited by S. Kai (Singapore: World Scientific).

22. T. Okuzono, and K. Kawasaki, Phys. Rev. E **51**, (1995) 1246.

23. D. Weaire, F. Bolton, T. Herdtle, and H. Aref, Phil. Mag. Lett. **66**,(1992) 293.

24. S. Hutzler, D. Weaire, and F. Bolton, Phil. Mag. B **71**, (1995) 277.

25. D. J. Durian, Phys. Rev. Lett. **75**, (1995) 4780.

26. D. J. Durian, Phys. Rev. E **55**, (1997) 1739.

27. Y. Jiang, P. J. Swart, A. Saxena, M. Asipauskas, and J. A. Glazier, Phys. Rev. E **59**, (1999) 5819.

28. S. Tewari, D. Schiemann, D. J. Durian, C. M. Knobler, S. A. Langer, and A. J. Liu, Phys. Rev. E **60**, (1999) 4385.

29. A. S. Argon, and H. Y. Kuo, Mat. Sci. and Eng. **39**, (1979) 101.

30. R. S. Ghaskadvi, and M. Dennin, Rev. Sci. Instr. **69**, (1998) 3568.

31. C. S. O'Hern, S. Langer, A. J. Liu, and S. R. Nagel, Phys. Rev. Lett. **88**, (2002) 075507.

32. C. S. O'Hern, S. Langer, A. J. Liu, and S. R. Nagel, Phys. Rev. Lett. **86**, (2001) 111.

33. C. S. O'Hern, L. E. Silbert, A. J. Liu, and S. R. Nagel, Phys. Rev. E **68**, (2003) 011306.
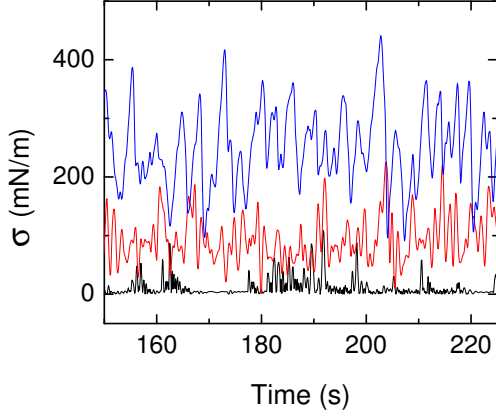
Fig. 1. A plot of stress on the inner cylinder versus time during steady rotation of the outer barrier. The characteristic stress relaxations are evident. The packing fractions for increasing average stress are 0.705 (black), 0.74 (red) and 0.78 (blue).
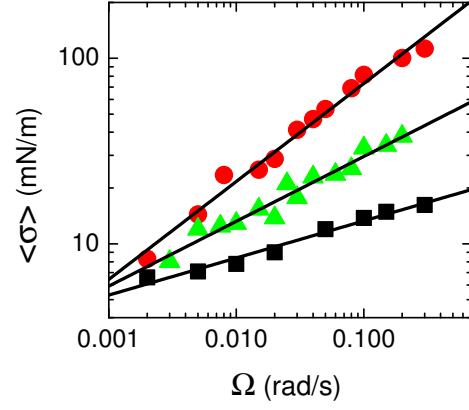

Fig. 2. A plot showing average stress values versus rotation rate for three different substrates: pure glycerine (•); 70 % glycerine/ 30 % water mixture (▲); and pure water (■). The solid lines indicate the consistency between the data and power law behavior.
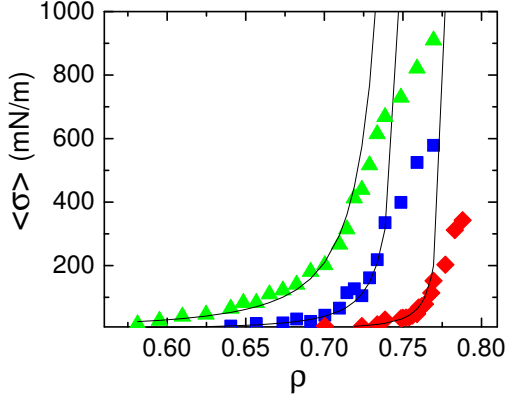
Fig. 3. A plot of the average stress value versus packing fraction for three different situations: rotation rate of 0.1 rad/s with pure glycerine substrate (▲); rotation rate of 0.02 rad/s with pure glycerine substrate (■); and rotation rate of 0.1 rad/s with pure water substrate (♦). The solid lines are a fits to Eq. 1, and they illustrate the diverging nature of the stress as the material is compressed.
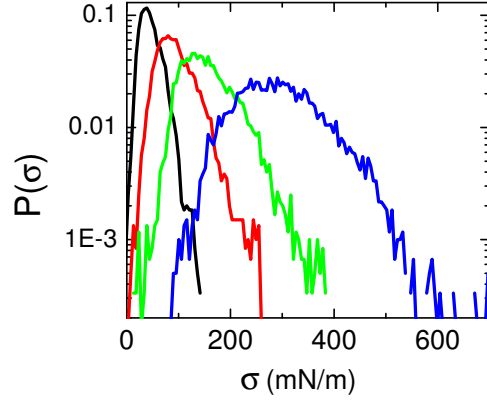
Fig. 4. A plot of the probability of a particular stress value for beads on pure water with a rotation rate of 0.1 rad/s. The four curves correspond to packing fractions of (in order of increasing mean): 0.71 (black); 0.74 (red); 0.75 (green); and 0.78 (blue).
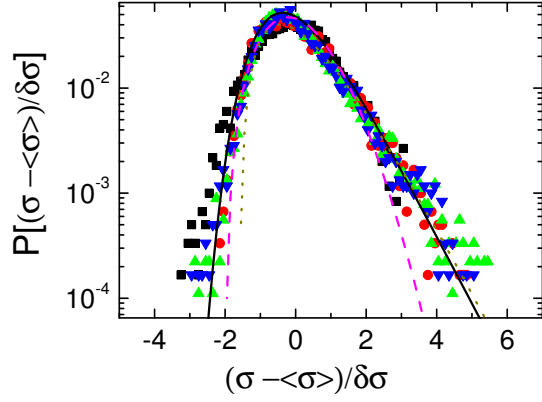
Fig. 5. The probability of $(\sigma - <\sigma>)/\delta\sigma$ is plotted, where $\delta\sigma$ is the standard deviation of the stress distribution. This is referred to as the normalized stress distribution. The different substrates and packing fractions are as follows: water substrate and packing fraction 0.71 (blue ▼); water substrate and packing fraction 0.77 (green ▲); packing fraction 0.68 and glycerine substrate (red ●); and a monodisperse system on water susbtrate (black ■). The lines are fits to three different possible distributions, as described in the text: the gFTG (solid line), two-dimensional Maxwell Boltzmann (dashed line), and one-dimensional Maxwell Boltzmann (dotted line)
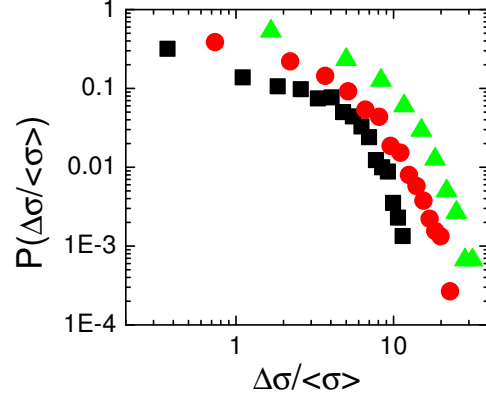
Fig. 6. A plot of the probability distribution for stress drops normalized by the average stress ($\Delta\sigma/<\sigma>$ for three different densities: $\rho = 0.735$ (▲); $\rho = 0.75$ (○); and $\rho = 0.765$ (■).
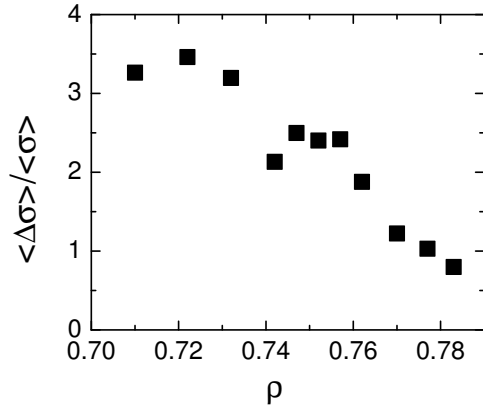
Fig. 7. A plot of the average stress drop, normalized by the average stress, $(< \Delta\sigma > / < \sigma >$ versus packing fraction. This is for the bidisperse system on water substrate.